Adaptive generalized matrix projective lag synchronization between two different complex networks with non-identical nodes and different dimensions

Dai Hao(戴 浩), Jia Li-Xin(贾立新)†, and Zhang Yan-Bin(张彦斌)

State Key Laboratory of Electrical Insulation and Power Equipment, School of Electrical Engineering, Xi'an Jiaotong University, Xi'an 710049, *China*

(Received 31 March 2012; revised manuscript received 27 April 2012)

The adaptive generalized matrix projective lag synchronization between two different complex networks with non-identical nodes and different dimensions is investigated in this paper. Based on Lyapunov stability theory and Barbalat's lemma, generalized matrix projective lag synchronization criteria are derived by using the adaptive control method. Furthermore, each network can be undirected or directed, connected or disconnected, and nodes in either network may have identical or different dynamics. The proposed strategy is applicable to almost all kinds of complex networks. In addition, numerical simulation results are presented to illustrate the effectiveness of this method, showing that the synchronization speed is sensitively influenced by the adaptive law strength, the network size, and the network topological structure.

Keywords: complex networks, generalized matrix projective lag synchronization, adaptive control, Lyapunov stability theory

PACS: 05.45.Xt, 05.45.Gg, 89.75.Hc **DOI:** 10.1088/1674-1056/21/12/120508

1. Introduction

A complex network is a large set of interconnected nodes, in which a node is a fundamental unit with specific contents. Complex networks are shown to exist in various fields of the real world, such as in the Internet, the World Wide Web, food webs, metabolic networks, linguistic networks, social networks, electricity distribution networks, etc. and thus become more and more important in our daily life. The nature of complex networks is the complexity, including topological structure, dynamical evolution, node diversity, and so on. Recently, due to the rapid development of computers, we are now able to quickly deal with large-scale data from networks, which has led to the discovery of "small-world networks" and "scale-free networks".[1,2] Consequently, complex networks become a focus point of research which has attracted increasing attention from various fields of science and engineering.

Among various complex dynamical behaviours, synchronization is a significant and interesting phenomenon. Pecora and Carroll[3] used the master stability function approach to determine the stability of the synchronous state in a coupled system. Wang and Chen[4,5] studied the synchronization in two specific kinds of networks: scale-free networks and small-world networks. Wu and Lu[6] studied the generalized projective synchronization between two different general complex dynamical networks with delayed coupling. In Refs. [7] and [8], the authors studied the synchronization between two different general complex dynamical networks with fractional-order chaos nodes. And then the pinning impulsive synchronization of stochastic delayed coupled networks was investigated by several other researchers in Ref. [9]. The synchronization within one network is named "inner synchronization", which is concerned with the synchronization among the nodes in a network. Different from the "inner synchronization", one may also consider "outer synchronization", which refers to the synchronization phenomenon between two or more complex networks regardless of the synchronization of the inner network, and it is always present in our lives. For instance, infectious diseases, such as AIDS, bird flu, and H1N1 influenza, were originally spread between two communities (or networks). This means that studying the dynamics between two coupled networks is necessary and important.

To the best of our knowledge, most existing pa-

†Corresponding author. E-mail: gongqi112@163.com

© 2012 Chinese Physical Society and IOP Publishing Ltd

pers discuss the synchronization between two different complex networks with identical or non-identical nodes that have the same dimensions.[10−15] However, in many real systems, the synchronization is carried out through the oscillators with different dimensions, especially the systems in biological science and social science. Therefore, the generalized matrix projective lag synchronization (GMPLS) between two different complex networks with different dimensions becomes a new meaningful problem. This paper focuses on the adaptive generalized matrix projective lag synchronization between two different complex networks with non-identical nodes and different dimensions. It expands the types of traditional synchronization and makes the scaling factor developing from a single value or diagonal matrix to a general matrix. Based on Lyapunov stability theory and Barbalat's lemma, some sufficient lag synchronization criteria are derived by using the adaptive control. The proposed strategy is applicable to almost all kinds of complex networks. Some examples are considered and their numerical simulations are performed. Numerical simulation results are presented to illustrate the effectiveness of this method.

The rest of the present paper is organized as follows. In Section 2 the network models and some useful preliminaries are given. In Section 3, by using the adaptive control method, some sufficient synchronization criteria are derived to guarantee GMPLS between two completely different complex dynamical networks with distinct nodes and different dimensions. In Section 4 some representative examples are used to validate the effectiveness of the proposed approach. Finally, some concluding remarks are drawn in Section 5.

2. Network models and preliminaries

2.1. Network models

Some necessary mathematical notations that are utilized throughout this paper are first introduced as follows. Let A^{T} (or x^{T}) be the transpose of the matrix A (or vector x). The $\|x\|$ denotes the 2-norm of the vector x. The $I_n \in R^{n\times n}$ represents the identity matrix with dimension n, the $\otimes$ denotes the Kronecker product of two matrices,[16] and $\lambda_{\max}(A)$ represents the maximum eigenvalue of a square matrix A.

Consider a general complex dynamical network consisting of N non-identical nodes with linear couplings, which is described by

$$\dot{x}_i(t) = A_i x_i(t) + f_i(x_i(t)) + \sum_{j=1}^{N} c_{ij} P x_j(t), \quad i = 1, 2, \ldots, N, \tag{1}$$

where $x_i = (x_{i1}, x_{i2}, \ldots, x_{in})^{\mathrm{T}} \in R^n$ is the state vector of the i-th node; $A_i \in R^{n\times n}$ is a constant matrix and $f_i : R^n \to R^n$ is a smooth nonlinear vector field; the nonlinear function $\varphi_i(\dot{x}_i(t)) = A_i x_i(t) + f_i(x_i(t))$ describes the dynamics of node i in the absence of interactions with other nodes; $P \in R^{n\times n}$ is the inner coupling matrix and $C = (c_{ij})_{N\times N} \in R^{N\times N}$ is the coupling configuration matrix representing the coupling strength and the topological structure of the network. The matrix C is defined as follows: if there exists a connection from node j to node i ($i \neq j$), then $c_{ij} \neq 0$; otherwise $c_{ij} = 0$. The diagonal elements of matrix C are defined by

$$c_{ii} = -\sum_{j=1, j\neq i}^{N} c_{ij}, \quad i = 1, 2, \ldots, N.$$

We take the network given by Eq. (1) as the drive network, and the response network with a nonlinear control scheme is given by

$$\dot{y}_i(t) = B_i y_i(t) + g_i(y_i(t)) + \sum_{j=1}^{N} d_{ij} Q y_j(t) + u_i(t), \quad i = 1, 2, \ldots, N, \tag{2}$$

where $y_i = (y_{i1}, y_{i2}, \ldots, y_{im})^{\mathrm{T}} \in R^m$ is the state vector of the i-th node; $B_i \in R^{m\times m}$ is the constant matrix and $g_i : R^m \to R^m$ is a smooth nonlinear vector field; $u_i(t) \in R^m$ are the adaptive controllers; $Q \in R^{m\times m}$ is the inner coupling matrix and $D = (d_{ij})_{N\times N} \in R^{N\times N}$ is the coupling configuration matrix, which has the same meaning as matrix C.

2.2. Preliminaries

In order to introduce our main results, the following definition and lemma are required.

Definition 1 Let $x_i(t - \tau(t))$ be the time delay state of node i in the drive network (1), and $y_i(t)$ be the current state of node i in the response network (2). Given the time-varying delay $\tau(t)$, if there exist the constant scaling matrix $M \in R^{m\times n}$ and $\|M\| \neq 0$ such that

$$\lim_{t\to\infty} \|y_i(t) - M x_i(t - \tau(t))\| = 0, \quad i = 1, 2, \ldots, N, \tag{3}$$

then it is said that we achieve generalized matrix projective lag synchronization (GMPLS) between networks (1) and (2) with $\tau(t) > 0$.

3. Synchronization criteria

In this section, we will study the GMPLS between two different complex networks with non-identical nodes and different dimensions by using the adaptive control method.

Define the synchronization errors as $e_i(t) = y_i(t) - Mx_i(t-\tau(t))$ $(i = 1, 2, \ldots, N)$, then the time derivative of $e_i(t)$ will be

$$\dot{e}_i(t) = \dot{y}_i(t) - M\dot{x}_i(t-\tau(t))(1-\dot{\tau}(t)), \quad i = 1, 2, \ldots, N. \tag{4}$$

By substituting Eqs. (1) and (2) into Eq. (4), we can obtain the error dynamical system as follows:

$$\begin{aligned}\dot{e}_i(t) = {} & B_i e_i(t) + (B_i M - MA_i)x_i(t-\tau(t)) \\ & + g_i(y_i(t)) - Mf_i(x_i(t-\tau(t))) \\ & + M\dot{x}_i(t-\tau(t))\dot{\tau}(t) + \sum_{j=1}^{N}(d_{ij}Qe_j(t) \\ & - \sum_{j=1}^{N}(c_{ij}MP - d_{ij}QM)x_j(t-\tau(t)) \\ & + u_i(t),\end{aligned} \tag{5}$$

where $i = 1, 2, \ldots, N$.

Theorem 1 Given the constant scaling matrix $M \in R^{m\times n}$ $(\|M\| \neq 0)$, the GMPLS between drive network (1) and response network (2) can be achieved by using the following adaptive controllers:

$$\begin{aligned}u_i(t) = {} & -(B_i M - MA_i)x_i(t-\tau(t)) - g_i(y_i(t)) \\ & + Mf_i(x_i(t-\tau(t))) - M\dot{x}_i(t-\tau(t))\dot{\tau}(t) \\ & + \sum_{j=1}^{N}(c_{ij}MP - d_{ij}QM)x_j(t-\tau(t)) - K_i e_i(t), \\ & i = 1, 2, \ldots, N,\end{aligned} \tag{6}$$

where K_i is a matrix of adaptive control parameters, and $K_i = \mathrm{diag}(k_{i1}, k_{i2}, \ldots, k_{im})$.

The adaptive laws of adaptive control parameters k_{ij} $(i = 1, 2, \ldots, N, j = 1, 2, \ldots, m)$ are designed as

$$\dot{k}_{ij} = \lambda\beta e_{ij}^2, \quad i = 1, 2, \ldots, N; j = 1, 2, \ldots, m, \tag{7}$$

where λ and β are constants larger than zero. They can adjust the amplitude of synchronization error and control the speed of convergence of synchronization error.

By substituting adaptive controller (6) into formula (5), the synchronization error dynamical system can be expressed as

$$\dot{e}_i(t) = B_i e_i(t) + \sum_{j=1}^{N} d_{ij}Qe_j(t) - K_i e_i(t), \quad i = 1, 2, \ldots, N. \tag{8}$$

Proof Let $e(t) = (e_1(t), e_2(t), \ldots, e_N(t))^{\mathrm{T}} \in R^{mN}$, $K_{ri} = (k_{i1}, k_{i2}, \ldots, k_{im})^{\mathrm{T}} \in R^m$, $I_r = (1, 1, \ldots, 1)^{\mathrm{T}} \in R^m$, $I \in R^{m\times m}$ is an identity matrix and construct the Lyapunov candidate function as follows:

$$\begin{aligned}V(t) = {} & \frac{1}{2}e^{\mathrm{T}}(t)e(t) \\ & + \sum_{i=1}^{N}\frac{1}{2\lambda\beta}(K_{ri} - \lambda I_r)^{\mathrm{T}}(K_{ri} - \lambda I_r).\end{aligned} \tag{9}$$

Obviously, $V(t) \geq 0$. Taking the time derivative of $V(t)$ along the trajectories of the synchronization error dynamical system (8), and using Eq. (6), we have

$$\begin{aligned}\dot{V}(t) = {} & \sum_{i=1}^{N} e_i^{\mathrm{T}}(t)\dot{e}_i(t) + \sum_{i=1}^{N}\frac{1}{2\lambda\beta}[\dot{K}_{ri}^{\mathrm{T}}(K_{ri} - \lambda I_r) \\ & + (K_{ri} - \lambda I_r)^{\mathrm{T}}\dot{K}_{ri}] \\ = {} & \sum_{i=1}^{N} e_i^{\mathrm{T}}(t)[B_i e_i(t) + \sum_{j=1}^{N} d_{ij}Qe_j(t) - K_i e_i(t)] \\ & + \sum_{i=1}^{N}\frac{1}{\lambda\beta}[(K_{ri} - \lambda I_r)^{\mathrm{T}}\dot{K}_{ri}] \\ = {} & \sum_{i=1}^{N} e_i^{\mathrm{T}}(t)B_i e_i(t) + \sum_{i=1}^{N}\sum_{j=1}^{N} d_{ij}e_i^{\mathrm{T}}(t)Qe_j(t) \\ & - \sum_{i=1}^{N} e_i^{\mathrm{T}}(t)K_i e_i(t) + \sum_{i=1}^{N} e_i^{\mathrm{T}}(t)(K_i - \lambda I)e_i(t) \\ = {} & \sum_{i=1}^{N} e_i^{\mathrm{T}}(t)B_i e_i(t) + \sum_{i=1}^{N}\sum_{j=1}^{N} d_{ij}e_i^{\mathrm{T}}(t)Qe_j(t) \\ & - \sum_{i=1}^{N} e_i^{\mathrm{T}}(t)\lambda I e_i(t) \\ \leq {} & (\lambda_{\max}\left(\frac{\hat{B} + \hat{B}^{\mathrm{T}}}{2}\right) \\ & + \lambda_{\max}\left(\frac{\hat{D} + \hat{D}^{\mathrm{T}}}{2}\right) - \lambda)e^{\mathrm{T}}(t)e(t),\end{aligned}$$

where $\hat{B} = \mathrm{diag}(B_1, B_2, \ldots, B_N) \in R^{mN\times mN}$, and $\hat{D} = D \otimes Q \in R^{mN\times mN}$.

If we choose

$$\lambda > \lambda^* = \lambda_{\max}\left(\frac{\hat{B} + \hat{B}^{\mathrm{T}}}{2}\right) + \lambda_{\max}\left(\frac{\hat{D} + \hat{D}^{\mathrm{T}}}{2}\right),$$

then we can obtain $\dot{V}(t) < 0$. On the basis of Barbalat's lemma,[17] one has $\lim_{t\to\infty} V(t) = 0$, i.e.,

$\lim_{t\to\infty} e_i(t) = 0$ $(i = 1, 2, \ldots, N)$. Therefore, the GMPLS between two different complex networks with non-identical nodes and different dimensions is asymptotically achieved by adaptive controller (6). This completes the proof.

Remark 1 In our work, the coupling configuration matrices C and D need not be symmetric or irreducible. In addition, there is not any constraint imposed on the inner coupling matrices P and Q. Furthermore, each node of the networks may have different local dynamics. The proposed approach is applicable to all kinds of complex dynamical networks.

Remark 2 The constant λ can be chosen appropriately beforehand to adjust the synchronization rate. Theoretically, a larger λ will lead to faster synchronization. However, the inequality $\lambda > \lambda^*$ is just a sufficient condition and not a necessary one.

4. Illustrative examples

In this section, some representative examples are performed to verify the effectiveness of the proposed synchronization scheme in the previous section. The following quantity:

$$E(t) = \sqrt{\sum_{i=1}^{N}\sum_{j=1}^{N} e_{ij}^2(t)/N}$$

is used to measure the quality of the synchronization process. It is obvious that when

$$\lim_{t\to\infty} E(t) = 0,$$

the drive and response networks achieve the desired synchronization globally.

In the simulations, drive network (1) is described by the following N different three-dimensional chaotic systems:[18]

$$\begin{bmatrix} \dot{x}_{i1}(t) \\ \dot{x}_{i2}(t) \\ \dot{x}_{i3}(t) \end{bmatrix} = \begin{bmatrix} -35 & 35 & 0 \\ 0 & 28 - \frac{1}{2}(i-1) & 0 \\ 0 & 0 & -8 \end{bmatrix} \begin{bmatrix} x_{i1}(t) \\ x_{i2}(t) \\ x_{i3}(t) \end{bmatrix} + \begin{bmatrix} -x_{i2}(t)x_{i3}(t) \\ (x_{i1}(t) - x_{i3}(t))^4 - 10x_{i1}(t)x_{i3}(t) \\ x_{i1}^2(t) + x_{i2}^2(t) \end{bmatrix}. \quad (10)$$

For response network (2), these nodes are described by the following four-dimensional hyperchaotic Chen systems:[19]

$$\begin{bmatrix} \dot{y}_{i1}(t) \\ \dot{y}_{i2}(t) \\ \dot{y}_{i3}(t) \\ \dot{y}_{i4}(t) \end{bmatrix} = \begin{bmatrix} -35 & 35 & 0 & 0 \\ 4 & 21 - \frac{1}{2}(i-1) & 0 & 4 \\ 0 & 0 & -3 & 0 \\ -2 & 0 & 0 & 0 \end{bmatrix} \begin{bmatrix} y_{i1}(t) \\ y_{i2}(t) \\ y_{i3}(t) \\ y_{i4}(t) \end{bmatrix} + \begin{bmatrix} 0 \\ -10y_{i1}(t)y_{i3}(t) \\ y_{i2}^2(t) \\ 0 \end{bmatrix}. \quad (11)$$

4.1. GMPLS between a star coupled network and a full coupled network

A star coupled network and a full coupled network are drawn in Fig. 1. The coupling configuration matrices are given respectively as follows:

$$C = \begin{bmatrix} -9 & 1 & 1 & 1 & 1 & 1 & 1 & 1 & 1 & 1 \\ 1 & -1 & 0 & 0 & 0 & 0 & 0 & 0 & 0 & 0 \\ 1 & 0 & -1 & 0 & 0 & 0 & 0 & 0 & 0 & 0 \\ 1 & 0 & 0 & -1 & 0 & 0 & 0 & 0 & 0 & 0 \\ 1 & 0 & 0 & 0 & -1 & 0 & 0 & 0 & 0 & 0 \\ 1 & 0 & 0 & 0 & 0 & -1 & 0 & 0 & 0 & 0 \\ 1 & 0 & 0 & 0 & 0 & 0 & -1 & 0 & 0 & 0 \\ 1 & 0 & 0 & 0 & 0 & 0 & 0 & -1 & 0 & 0 \\ 1 & 0 & 0 & 0 & 0 & 0 & 0 & 0 & -1 & 0 \\ 1 & 0 & 0 & 0 & 0 & 0 & 0 & 0 & 0 & -1 \end{bmatrix},$$

$$D = \begin{bmatrix} -9 & 1 & 1 & 1 & 1 & 1 & 1 & 1 & 1 & 1 \\ 1 & -9 & 1 & 1 & 1 & 1 & 1 & 1 & 1 & 1 \\ 1 & 1 & -9 & 1 & 1 & 1 & 1 & 1 & 1 & 1 \\ 1 & 1 & 1 & -9 & 1 & 1 & 1 & 1 & 1 & 1 \\ 1 & 1 & 1 & 1 & -9 & 1 & 1 & 1 & 1 & 1 \\ 1 & 1 & 1 & 1 & 1 & -9 & 1 & 1 & 1 & 1 \\ 1 & 1 & 1 & 1 & 1 & 1 & -9 & 1 & 1 & 1 \\ 1 & 1 & 1 & 1 & 1 & 1 & 1 & -9 & 1 & 1 \\ 1 & 1 & 1 & 1 & 1 & 1 & 1 & 1 & -9 & 1 \\ 1 & 1 & 1 & 1 & 1 & 1 & 1 & 1 & 1 & -9 \end{bmatrix}.$$

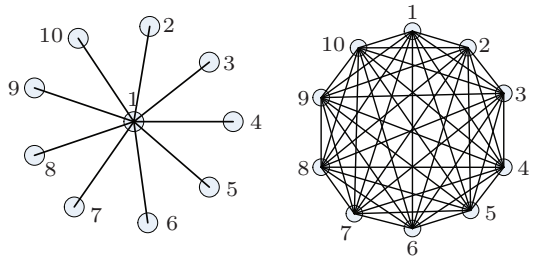


Fig. 1. (Left) a star coupled network and (right) a full coupled network.

The inner coupling matrices are taken arbitrarily as

$$P = \mathrm{diag}(0.1, 0.2, 0.3) \text{ and } Q = \mathrm{diag}(0.5, 0.1, 0.2, 0.3).$$

It is easy to obtain $\lambda_{\max}[(\hat{B} + \hat{B}^{\mathrm{T}})/2] = 27.2163$ and $\lambda_{\max}[(\hat{D} + \hat{D}^{\mathrm{T}})/2] = 6.3564 \times 10^{-16}$. Thus we obtain $\lambda^* = 27.2163$. We arbitrarily choose $N = 10$, $\lambda = 30$, and $\beta = 0.01$.

Example 1 We arbitrarily choose $\tau(t) = 0.1$,

$$M = \begin{bmatrix} 1 & 0 & 1 \\ 1 & 1 & 0 \\ 0 & 1 & 1 \\ 1 & 1 & 1 \end{bmatrix}.$$

Figure 2 displays the time evolutions of the synchronization errors $e_i(t)$ and $E(t)$ with $\tau(t) = 0.1$, $\beta = 0.01$, and $\lambda = 30$, which indicates that GMPLS between the star coupled network and the full coupled network is achieved. When $\tau(t) = 0.1$, Fig. 3 displays the values of synchronization error $E(t)$ for different values of λ and β. From Fig. 3, one can find that the larger the adaptive law strength λ or β, the faster the desired GMPLS is achieved. Furthermore, Fig. 3 shows that the synchronization rate is sensitively influenced by the adaptive law strength β, which is stronger than λ.

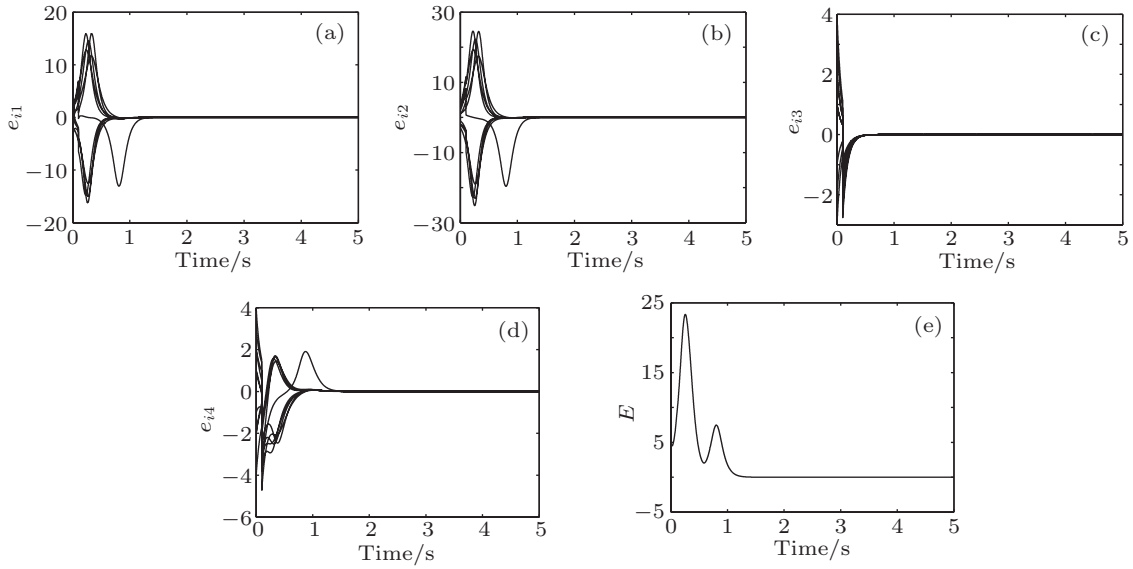


Fig. 2. The GMPLS errors between the star coupled network and the full coupled network varying with time: (a) GMPLS errors e_{i1}. (b) GMPLS errors e_{i2}. (c) GMPLS errors e_{i3}. (d) GMPLS errors e_{i4}. (e) Synchronization error $E(t)$.

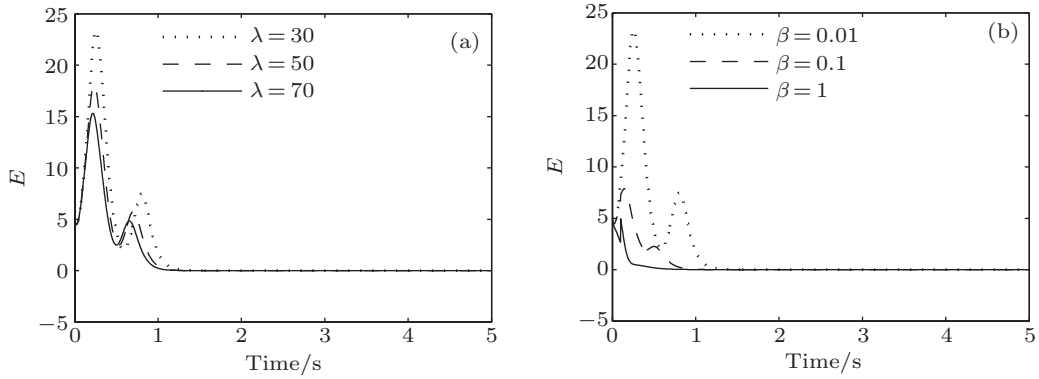


Fig. 3. Values of synchronization error $E(t)$ versus time for different values of λ (a) and β (b).

Example 2 We arbitrarily choose $\tau(t) = 0.2 - 0.01\sin(2t)$,

$$M = \begin{bmatrix} 2 & 1.6 & 3 \\ -1 & 2 & 1 \\ 0.5 & -1 & 1.8 \\ 1 & 0 & 0.2 \end{bmatrix}.$$

Figure 4 displays the time evolutions of the synchronization errors $e_i(t)$ and $E(t)$ with

$$\tau(t) = 0.2 - 0.01\sin(2t),$$

$\beta = 0.01$, and $\lambda = 30$, which indicates that GMPLS between the star coupled network and the full coupled network is achieved. When $\tau(t) = 0.2 - 0.01\sin(2t)$, Fig. 5 displays the values of synchronization error $E(t)$ for different values of λ and β. From Fig. 5, one can find that the larger the adaptive law strength λ or β, the faster the desired GMPLS is achieved. Furthermore, Fig. 5 shows that the synchronization rate is sensitively influenced by the adaptive law strength β, which is stronger than λ.

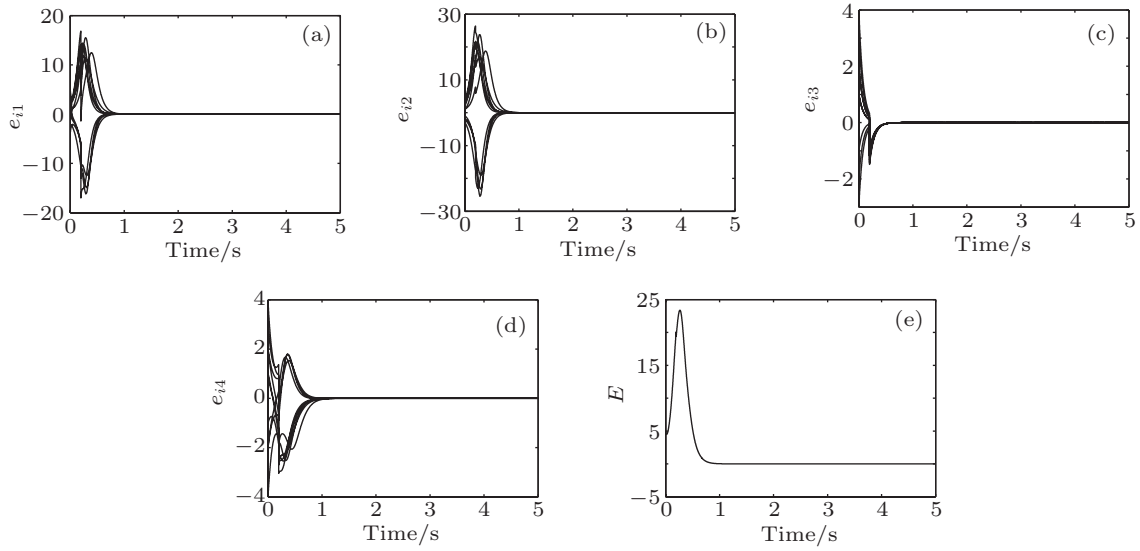


Fig. 4. The GMPLS errors between the star coupled network and the full coupled network varying with time: (a) GMPLS errors e_{i1}. (b) GMPLS errors e_{i2}. (c) GMPLS errors e_{i3}. (d) GMPLS errors e_{i4}. (e) Synchronization error $E(t)$.

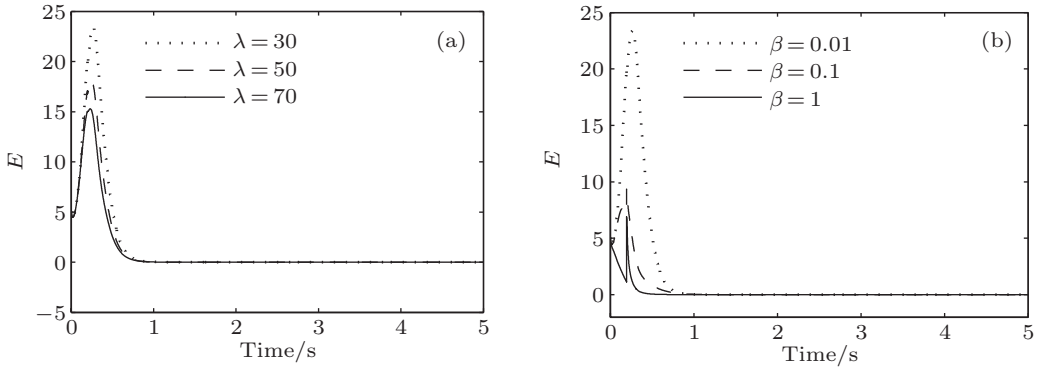


Fig. 5. Values of synchronization error $E(t)$ versus time for different values of λ (a) and β (b).

4.2. GMPLS between a tree network and a directed ring network

A tree network and a directed ring network are drawn in Fig. 6. The coupling configuration matrices are given respectively as follows:

$$C = \begin{bmatrix} -3 & 1 & 1 & 1 & 0 & 0 & 0 & 0 & 0 & 0 \\ 1 & -3 & 0 & 0 & 1 & 1 & 0 & 0 & 0 & 0 \\ 1 & 0 & -3 & 0 & 0 & 0 & 1 & 1 & 0 & 0 \\ 1 & 0 & 0 & -3 & 0 & 0 & 0 & 0 & 1 & 1 \\ 0 & 1 & 0 & 0 & -1 & 0 & 0 & 0 & 0 & 0 \\ 0 & 1 & 0 & 0 & 0 & -1 & 0 & 0 & 0 & 0 \\ 0 & 0 & 1 & 0 & 0 & 0 & -1 & 0 & 0 & 0 \\ 0 & 0 & 1 & 0 & 0 & 0 & 0 & -1 & 0 & 0 \\ 0 & 0 & 0 & 1 & 0 & 0 & 0 & 0 & -1 & 0 \\ 0 & 0 & 0 & 1 & 0 & 0 & 0 & 0 & 0 & -1 \end{bmatrix},$$

$$D = \begin{bmatrix} -1 & 0 & 0 & 0 & 0 & 0 & 0 & 0 & 0 & 1 \\ 1 & -1 & 0 & 0 & 0 & 0 & 0 & 0 & 0 & 0 \\ 0 & 1 & -1 & 0 & 0 & 0 & 0 & 0 & 0 & 0 \\ 0 & 0 & 1 & -1 & 0 & 0 & 0 & 0 & 0 & 0 \\ 0 & 0 & 0 & 1 & -1 & 0 & 0 & 0 & 0 & 0 \\ 0 & 0 & 0 & 0 & 1 & -1 & 0 & 0 & 0 & 0 \\ 0 & 0 & 0 & 0 & 0 & 1 & -1 & 0 & 0 & 0 \\ 0 & 0 & 0 & 0 & 0 & 0 & 1 & -1 & 0 & 0 \\ 0 & 0 & 0 & 0 & 0 & 0 & 0 & 1 & -1 & 0 \\ 0 & 0 & 0 & 0 & 0 & 0 & 0 & 0 & 1 & -1 \end{bmatrix}.$$

The inner coupling matrices are taken arbitrarily as $P = \mathrm{diag}(1, 1, 1)$ and $Q = \mathrm{diag}(2, 1, 3, 4)$. It is easy to obtain $\lambda_{\max}[(\hat{B} + \hat{B}^{\mathrm{T}})/2] = 27.2163$ and $\lambda_{\max}[(\hat{D} + \hat{D}^{\mathrm{T}})/2] = 2.9218 \times 10^{-15}$. Thus we obtain $\lambda^* = 27.2163$. We arbitrarily choose $N = 10$, $\lambda = 30$, and $\beta = 0.01$.

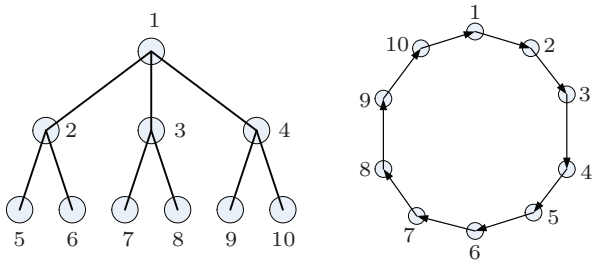


Fig. 6. (Left) a tree network and (right) a directed ring network.

Example 3 We arbitrarily choose $\tau(t) = 0.2$,

$$M = \begin{bmatrix} 1 & -1 & 2 \\ 3 & 5 & -3 \\ 2 & -1 & 4 \\ 5 & 0 & -2 \end{bmatrix}.$$

Figure 7 displays the time evolutions of the synchronization errors $e_i(t)$ and $E(t)$ with $\tau(t) = 0.2$, $\beta = 0.01$, and $\lambda = 30$, which indicates that GMPLS between the tree network and the directed ring network is achieved. When $\tau(t) = 0.2$, Fig. 8 displays the values of synchronization error $E(t)$ versus time for different values of λ and β. From Fig. 8, one can find that the larger the adaptive law strength λ or β, the faster the desired GMPLS is achieved. Furthermore, Fig. 8 shows that the synchronization rate is sensitively influenced by the adaptive law strength β, which is stronger than λ.

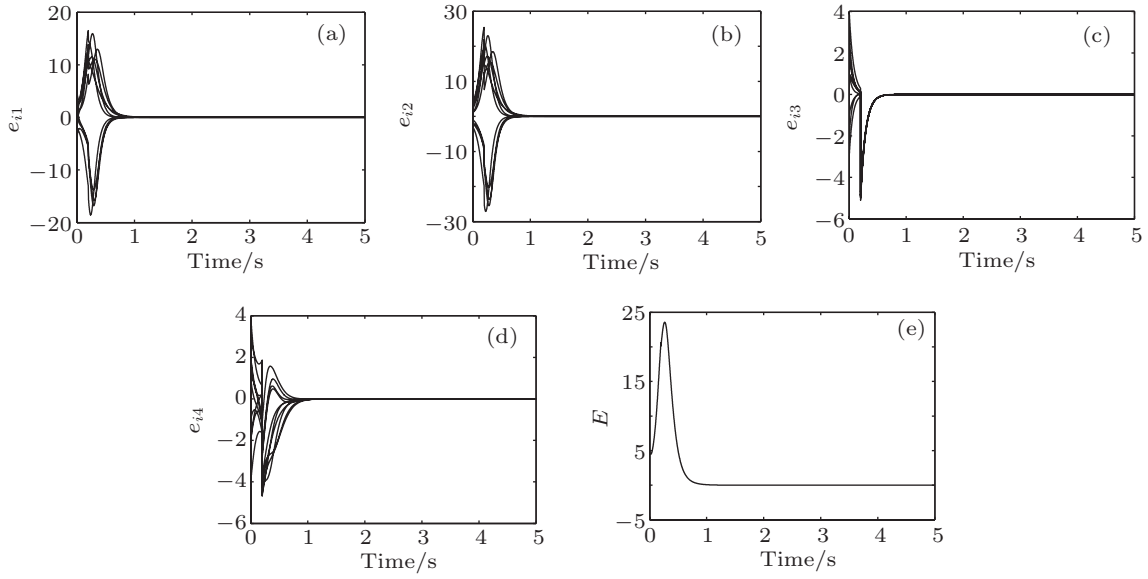


Fig. 7. The GMPLS errors between the tree network and the directed ring network varying with time: (a) GMPLS errors e_{i1}. (b) GMPLS errors e_{i2}. (c) GMPLS errors e_{i3}. (d) GMPLS errors e_{i4}. (e) Synchronization error $E(t)$.

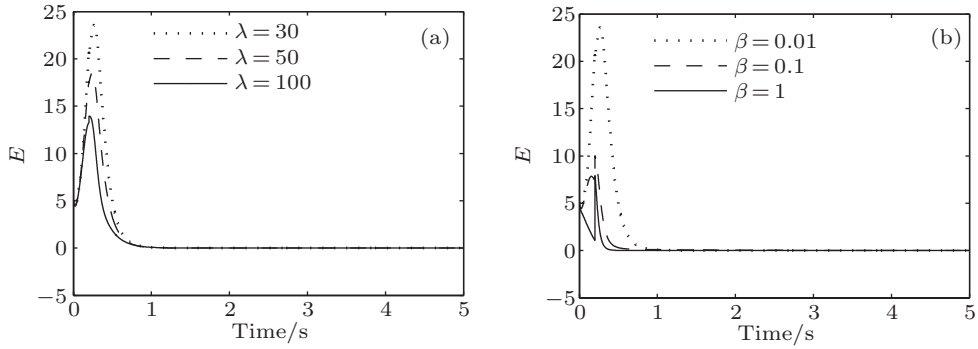


Fig. 8. Values of synchronization error $E(t)$ versus time for different values of λ (a) and β (b).

Example 4 We arbitrarily choose $\tau(t) = 0.1 - 0.02\cos(3t)$, $M = \begin{bmatrix} 1 & -1 & 2 \\ 3 & 5 & -3 \\ 2 & -1 & 4 \\ 5 & 0 & -2 \end{bmatrix}$.

Figure 9 displays the time evolutions of the synchronization errors $e_i(t)$ and $E(t)$ with $\tau(t) = 0.1 - 0.02\cos(3t)$, $\beta = 0.01$, and $\lambda = 30$, which indicates that GMPLS between the tree network and the directed ring network is achieved. When $\tau(t) = 0.1 - 0.02\cos(3t)$, Fig. 10 displays the values of synchronization error $E(t)$ versus time for different values of λ and β. From Fig. 10, one can find that the larger the adaptive law strength λ or β, the faster the desired GMPLS is achieved. Furthermore, Fig. 10 shows that the synchronization rate is sensitively influenced by the adaptive law strength β, which is stronger than λ.

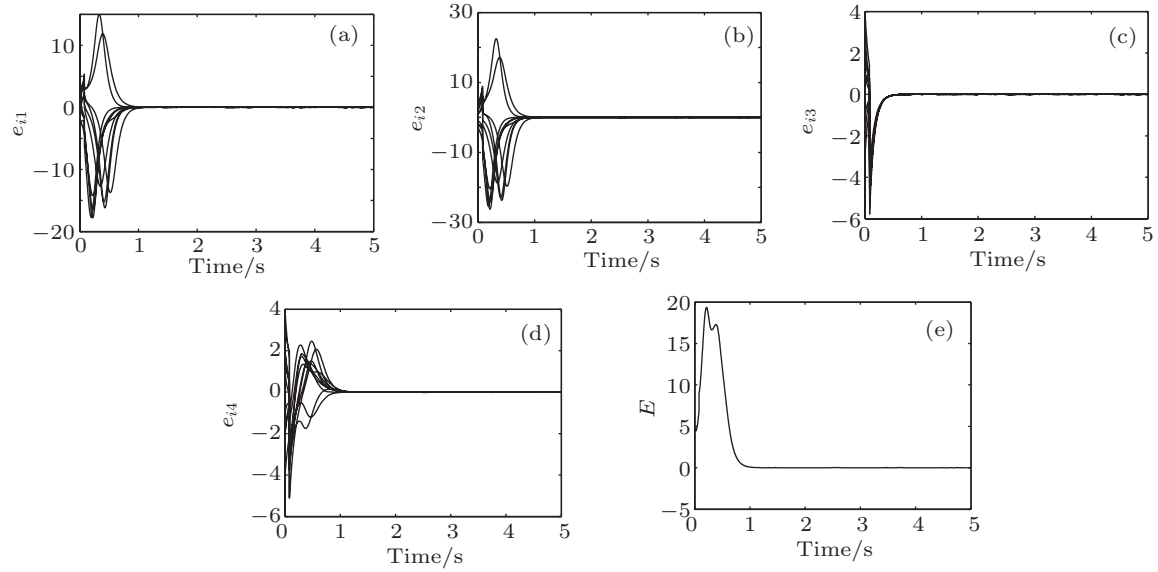


Fig. 9. The GMPLS errors between the tree network and the directed ring network varying with time: (a) GMPLS errors e_{i1}. (b) GMPLS errors e_{i2}. (c) GMPLS errors e_{i3}. (d) GMPLS errors e_{i4}. (e) The synchronization error $E(t)$.

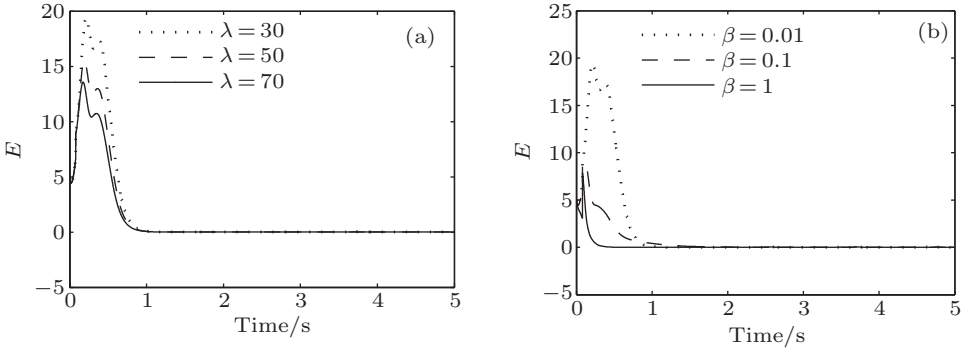


Fig. 10. Values of synchronization error $E(t)$ versus time for different values of λ (a) and β (b).

4.3. GMPLS between two directed complex networks

Two different directed complex networks are drawn in Fig. 11. The coupling configuration matrices are given respectively as follows:

$$C = \begin{bmatrix} -4 & 0 & 1 & 1 & 0 & 0 & 1 & 0 & 1 & 0 \\ 0 & -2 & 0 & 0 & 0 & 1 & 0 & 0 & 1 & 0 \\ 1 & 0 & -3 & 0 & 0 & 0 & 1 & 0 & 0 & 1 \\ 0 & 1 & 0 & -2 & 0 & 0 & 0 & 1 & 0 & 0 \\ 1 & 0 & 1 & 0 & -5 & 1 & 0 & 1 & 1 & 0 \\ 0 & 0 & 0 & 0 & 1 & -1 & 0 & 0 & 0 & 0 \\ 1 & 0 & 0 & 0 & 1 & 0 & -3 & 0 & 0 & 1 \\ 0 & 0 & 1 & 0 & 1 & 0 & 0 & -3 & 1 & 0 \\ 0 & 1 & 0 & 0 & 0 & 0 & 1 & 0 & -2 & 0 \\ 0 & 1 & 0 & 1 & 0 & 1 & 0 & 0 & 1 & -4 \end{bmatrix},$$

$$D = \begin{bmatrix} -2 & 0 & 1 & 0 & 0 & 1 & 0 & 0 & 0 & 0 \\ 0 & -3 & 0 & 1 & 0 & 1 & 0 & 1 & 0 & 0 \\ 1 & 0 & -3 & 0 & 0 & 0 & 1 & 0 & 1 & 0 \\ 0 & 1 & 0 & -4 & 0 & 1 & 0 & 1 & 0 & 1 \\ 0 & 0 & 1 & 0 & -3 & 0 & 1 & 0 & 0 & 1 \\ 0 & 0 & 0 & 1 & 0 & -2 & 0 & 0 & 1 & 0 \\ 1 & 0 & 0 & 0 & 1 & 0 & -3 & 1 & 0 & 0 \\ 0 & 1 & 0 & 1 & 0 & 1 & 0 & -4 & 0 & 1 \\ 0 & 0 & 1 & 0 & 0 & 0 & 0 & 1 & -2 & 0 \\ 1 & 0 & 0 & 1 & 1 & 0 & 1 & 0 & 1 & -5 \end{bmatrix}.$$

The inner coupling matrices are taken arbitrarily as $P = \mathrm{diag}(1, 2, 3)$ and $Q = \mathrm{diag}(0.1, 2, 0.3, 1)$. It is easy to obtain $\lambda_{\max}[(\hat{B} + \hat{B}^{\mathrm{T}})/2] = 27.2163$ and $\lambda_{\max}[(\hat{D} + \hat{D}^{\mathrm{T}})/2] = 0.2368$. Thus we obtain $\lambda^* = 27.4532$. We arbitrarily choose $N = 10$, $\lambda = 30$, and $\beta = 0.01$.

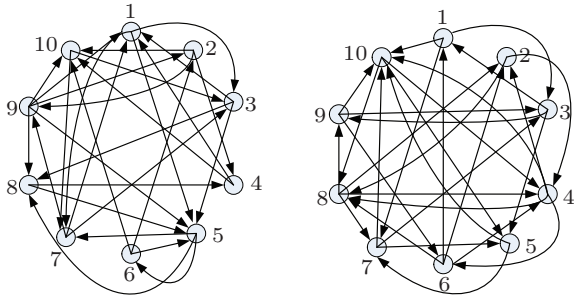


Fig. 11. Two different directed complex networks.

Example 5 We arbitrarily choose $\tau(t) = 0.15$,

$$M = \begin{bmatrix} 1 & 2 & 3 \\ 3 & -1 & 1 \\ 1 & -2 & 4 \\ -3 & 5 & 0 \end{bmatrix}.$$

Figure 12 displays the time evolutions of the synchronization errors $e_i(t)$ and $E(t)$ with $\tau(t) = 0.15$, $\beta = 0.01$, and $\lambda = 30$, which indicates that GMPLS between two different directed complex networks is achieved. When $\tau(t) = 0.15$, Fig. 13 displays the values of synchronization error $E(t)$ versus time for different values of λ and β. From Fig. 13, one can find that the larger the adaptive law strength λ or β, the faster the desired GMPLS is achieved. Furthermore, Fig. 13 shows that the synchronization rate is sensitively influenced by the adaptive law strength β, which is stronger than λ.

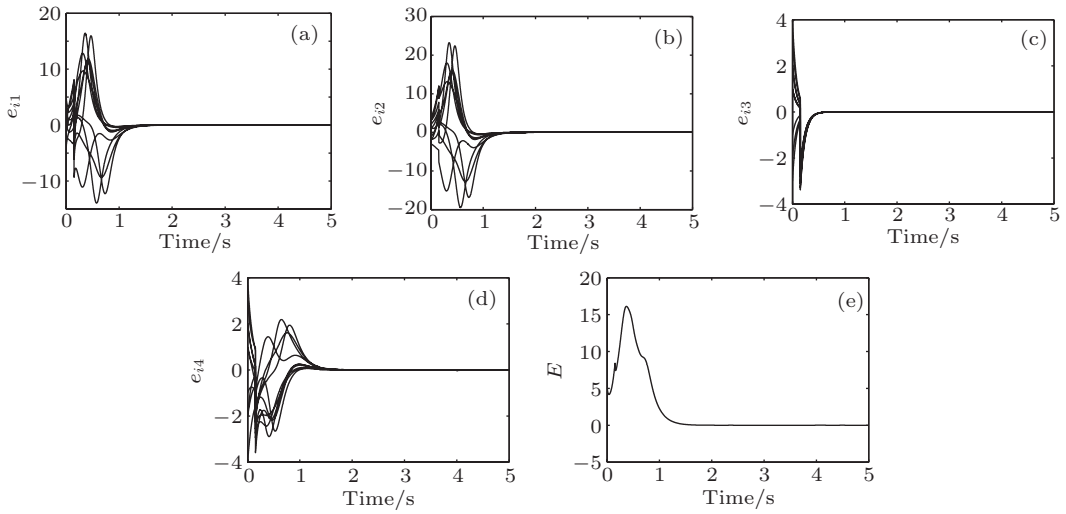


Fig. 12. The GMPLS errors between two different directed complex networks varying with time: (a) GMPLS errors e_{i1}. (b) GMPLS errors e_{i2}. (c) GMPLS errors e_{i3}. (d) GMPLS errors e_{i4}. (e) The synchronization error $E(t)$.

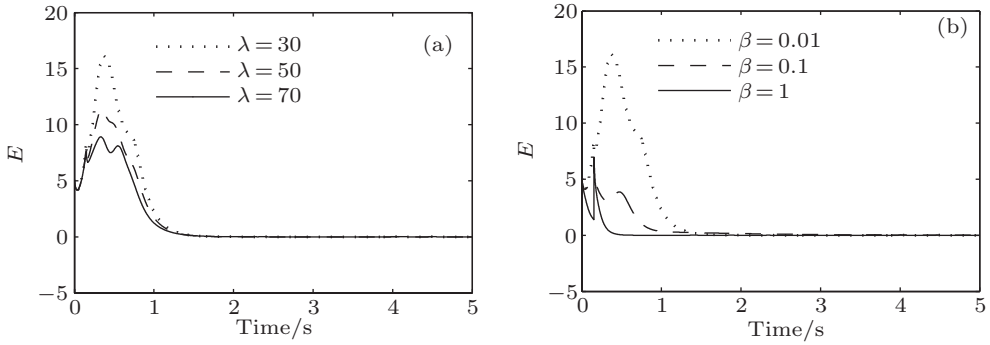


Fig. 13. Values of synchronization error $E(t)$ versus time for different values of λ (a) and β (b).

Example 6 We arbitrarily choose $\tau(t) = 0.15 - 0.01(\sin(2t)\cos(3t))$, $M = \begin{bmatrix} 1 & 2 & 3 \\ 3 & -1 & 1 \\ 1 & -2 & 4 \\ -3 & 5 & 0 \end{bmatrix}$.

Figure 14 displays the time evolutions of the synchronization errors $e_i(t)$ and $E(t)$ with $\tau(t) = 0.15 - 0.01(\sin(2t)\cos(3t))$, $\beta = 0.01$, and $\lambda = 30$, which indicates that GMPLS between two different directed complex networks is achieved. When $\tau(t) = 0.15 - 0.01(\sin(2t)\cos(3t))$, Fig. 15 displays the values of synchronization error $E(t)$ versus time for different values of λ and β. From Fig. 15, one can find that the larger the adaptive law strength λ or β, the faster the desired GMPLS is achieved. Furthermore, Fig. 15 shows that the synchronization rate is sensitively influenced by the adaptive law strength β, which is stronger than λ.

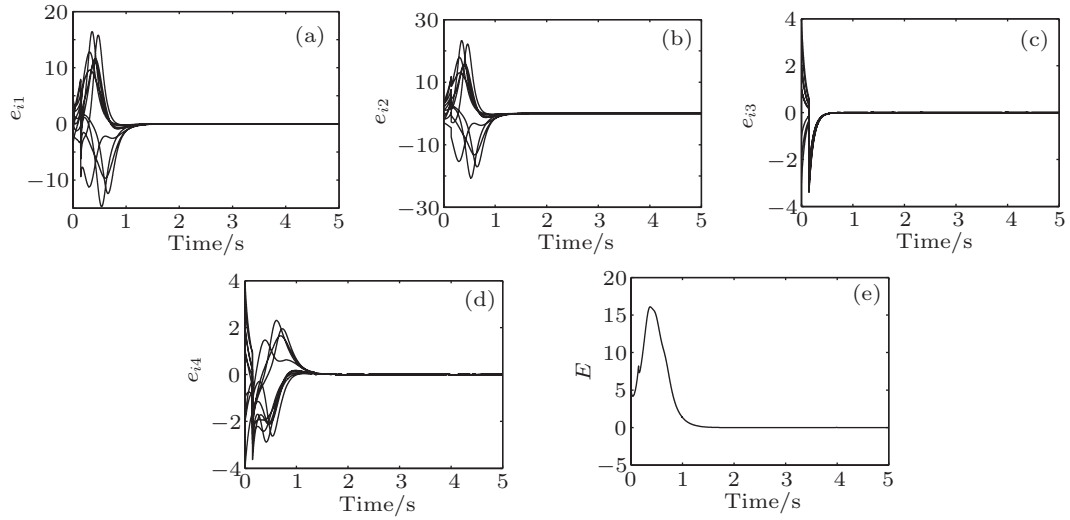


Fig. 14. The GMPLS errors between two different directed complex networks varying with time: (a) GMPLS errors e_{i1}. (b) GMPLS errors e_{i2}. (c) GMPLS errors e_{i3}. (d) GMPLS errors e_{i4}. (e) The synchronization error $E(t)$.

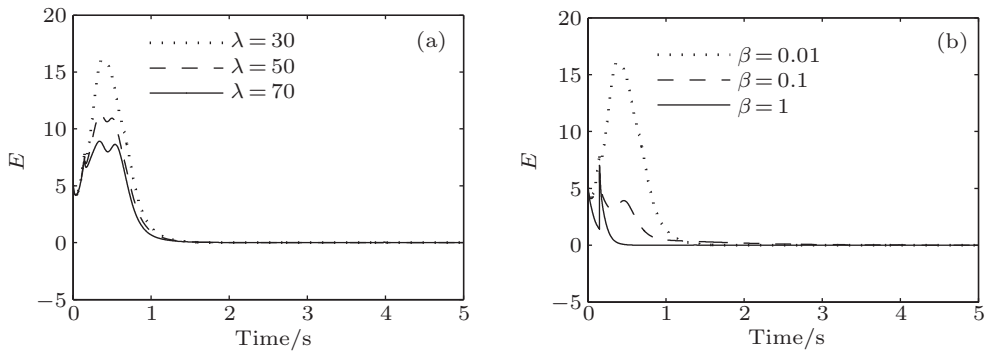


Fig. 15. Values of synchronization error $E(t)$ versus time for different values of λ (a) and β (b).

4.4. GMPLS between a star coupled network and a full coupled network with $N = 6$

A star coupled network and a full coupled network with $N = 6$ are drawn in Fig. 16. The coupling configuration matrices are given respectively as follows:

$$C = \begin{bmatrix} -5 & 1 & 1 & 1 & 1 & 1 \\ 1 & -1 & 0 & 0 & 0 & 0 \\ 1 & 0 & -1 & 0 & 0 & 0 \\ 1 & 0 & 0 & -1 & 0 & 0 \\ 1 & 0 & 0 & 0 & -1 & 0 \\ 1 & 0 & 0 & 0 & 0 & -1 \end{bmatrix},$$

$$D = \begin{bmatrix} -5 & 1 & 1 & 1 & 1 & 1 \\ 1 & -5 & 1 & 1 & 1 & 1 \\ 1 & 1 & -5 & 1 & 1 & 1 \\ 1 & 1 & 1 & -5 & 1 & 1 \\ 1 & 1 & 1 & 1 & -5 & 1 \\ 1 & 1 & 1 & 1 & 1 & -5 \end{bmatrix}.$$

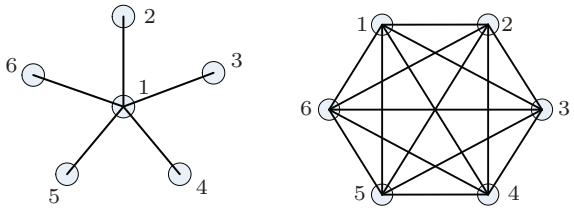


Fig. 16. (Left) A star coupled network and (right) a full coupled network.

The inner coupling matrices are taken arbitrarily as

$$P = \mathrm{diag}(0.1, 0.2, 0.3) \text{ and } Q = \mathrm{diag}(0.5, 0.1, 0.2, 0.3).$$

It is easy to obtain $\lambda_{\max}[(\hat{B} + \hat{B}^{\mathrm{T}})/2] = 27.2163$ and $\lambda_{\max}[(\hat{D} + \hat{D}^{\mathrm{T}})/2] = -0.4$. Thus we obtain $\lambda^* = 26.8163$. We arbitrarily choose $\lambda = 30$ and $\beta = 0.01$.

Example 7 We arbitrarily choose $\tau(t) = 0.1$ and $\tau(t) = 0.2 - 0.01\sin(2t)$, respectively, $M = \begin{bmatrix} 1 & 0 & 1 \\ 1 & 1 & 0 \\ 0 & 1 & 1 \\ 1 & 1 & 1 \end{bmatrix}$.

When $\tau(t) = 0.1$ and $\tau(t) = 0.2 - 0.01\sin(2t)$, the values of synchronization error $E(t)$ versus time for different values of N are shown in Figs. 17(a) and 17(b), respectively.

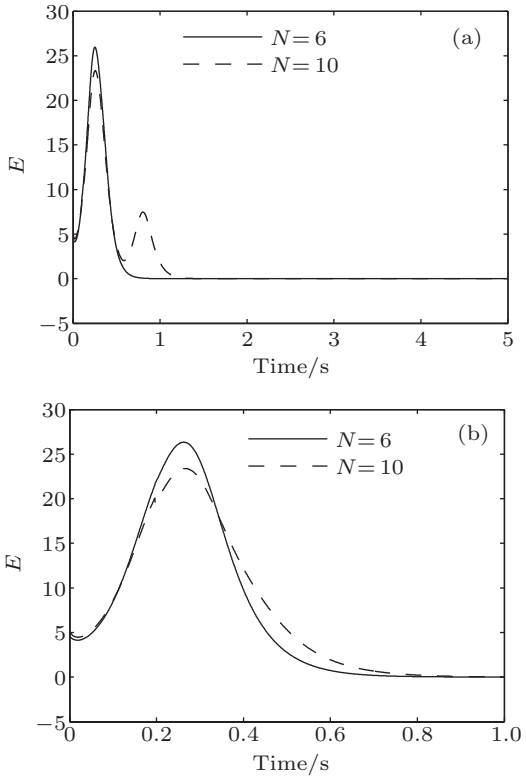


Fig. 17. Values of synchronization error $E(t)$ versus time for different values of N: (a) $\tau(t) = 0.1$, (b) $\tau(t) = 0.2 - 0.01\sin(2t)$.

Seven examples in four groups are simulated to verify the effectiveness of the proposed synchronization method in this paper. The first two examples in group one are performed to illustrate that the proposed synchronization method can adapt to the synchronization for two undirected coupled networks. The following two examples in group two are performed to illustrate that the proposed method can adapt to the synchronization between an undirected coupled network and a directed coupled network. Examples five and six in group three are performed to illustrate that the proposed method can adapt to the synchronization for directed coupled networks. The last example in group four is performed to illustrate that the synchronization speed is influenced by the network size. Four representative and regular networks (a star coupled network, a full coupled network, a tree network, and a directed ring network) are used to verify the effectiveness of the proposed method in the first two groups. However, two irregular and directed coupled complex networks are used to verify the effectiveness of the proposed method in the third group. This group of experiments have more generality, representation, and more suitable to illustrate the effectiveness of the proposed method.

From the above numerical simulation results, the limit of the synchronization error $E(t)$ asymptotically approaches to zero. That is to say, through the adaptive control method, generalized matrix projective lag synchronization between two completely different complex dynamical networks with non-identical nodes and different dimensions can be accomplished. In addition, it indicates that the time delay $\tau(t)$ has little influence on synchronization speed; however, the synchronization speed is sensitively influenced by the adaptive law strength, the network size, and the network topological structure.

5. Conclusions

In this paper, we investigated generalized matrix projective lag synchronization between two completely different complex dynamical networks with non-identical nodes and different dimensions. According to the Lyapunov stability theory and Barbalat's lemma, we proposed an adaptive control scheme to achieve GMPLS. The coupling configuration matrix is not necessarily symmetric or irreducible. In addition, there is no constraint imposed on the inner coupling matrix. The presented method can be applied to a great variety of complex dynamical networks. Some representative examples are provided to show the effectiveness and feasibility of the proposed synchronization method. Numerical simulation results show that the synchronization speed is sensitively influenced by the adaptive law strength, the network size, and the network topological structure.

References

[1] Watts D J and Strogatz S H 1998 *Nature* **391** 440

[2] Barabasi A L and Albert R 1999 *Science* **286** 509

[3] Pecora L M and Carroll T L 1998 *Phys. Rev. Lett.* **80** 2109

[4] Wang X F and Chen G R 2002 *Int. J. Bifur. Chaos* **12** 187.

[5] Wang X F and Chen G R 2002 *IEEE Trans. Circ. Syst.* I **49** 54

[6] Wu X J and Lu H T 2010 *Phys. Lett.* A **374** 3932

[7] Wu X J and Lu H T 2010 *Chin. Phys.* B **19** 070511

[8] Wang M J, Wang X Y and Niu Y J 2011 *Chin. Phys.* B **20** 010508

[9] Tang Y, Wong W K, Fang J A and Miao Q Y 2011 *Chin. Phys.* B **20** 040513

[10] Zheng S, Bi Q S and Cai G L 2009 *Phys. Lett.* A **373** 1553

[11] Tang H W, Chen L, Lu J A and Tse C K 2008 *Phys. Lett.* A **387** 5623

[12] Chen B R, Jiao L C, Wu J S and Wang X H 2009 *Chin. Phys. Lett.* **26** 060505

[13] Zhou J, Lu J A and Lü J H 2008 *Automatica* **44** 996

[14] Yu W W, Chen G R and Lü J H 2009 *Automatica* **45** 429

[15] Wen S, Chen S H and Guo W L 2008 *Phys. Lett.* A **372** 6340

[16] Regalia P A and Sanjit M K 1989 *SIAM Rev.* **31** 586

[17] Wu X J and Lu H T 2012 *Commun. Nonlinear Sci. Numer. Simulat.* **17** 3005

[18] Dai H, Jia L X, Hui M and Si G Q 2011 *Chin. Phys.* B **20** 040507

[19] Jia L X, Dai H and Hui M 2010 *Chin. Phys.* B **19** 100501